doi:10.1093/brain/awu214 Brain 2014: 137; 2690–2702 | 2690

BRAIN
A JOURNAL OF NEUROLOGY

Resilience of developing brain networks to interictal epileptiform discharges is associated with cognitive outcome

George M. Ibrahim,[1,2] Daniel Cassel,[3] Benjamin R. Morgan,[4] Mary Lou Smith,[5] Hiroshi Otsubo,[6] Ayako Ochi,[6] Margot Taylor,[3,4,5] James T. Rutka,[1] O. Carter Snead III[2,3,6] and Sam Doesburg[2,3,4,5]

1 Division of Neurosurgery, Hospital for Sick Children, Department of Surgery, University of Toronto, Toronto, Ontario, Canada
2 Institute of Medical Science, University of Toronto, Toronto, Ontario, Canada
3 Neuroscience and Mental Health Program, Hospital for Sick Children Research Institute, Toronto, Ontario, Canada
4 Department of Diagnostic Imaging, Hospital for Sick Children, Toronto, Ontario, Canada
5 Department of Psychology, University of Toronto, Toronto, Ontario, Canada
6 Division of Neurology, Hospital for Sick Children, University of Toronto, Toronto, Ontario, Canada

Correspondence to: George M. Ibrahim, MD, PhD,
Division of Neurosurgery,
The Hospital for Sick Children,
555 University Avenue,
Toronto ON, M5G 1Z8
E-mail: georgem.ibrahim@utoronto.ca

The effects of interictal epileptiform discharges on neurocognitive development in children with medically-intractable epilepsy are poorly understood. Such discharges may have a deleterious effect on the brain's intrinsic connectivity networks, which reflect the organization of functional networks at rest, and in turn on neurocognitive development. Using a combined functional magnetic resonance imaging–magnetoencephalography approach, we examine the effects of interictal epileptiform discharges on intrinsic connectivity networks and neurocognitive outcome. Functional magnetic resonance imaging was used to determine the location of regions comprising various intrinsic connectivity networks in 26 children (7–17 years), and magnetoencephalography data were reconstructed from these locations. Inter-regional phase synchronization was then calculated across interictal epileptiform discharges and graph theoretical analysis was applied to measure event-related changes in network topology in the peri-discharge period. The magnitude of change in network topology (network resilience/vulnerability) to interictal epileptiform discharges was associated with neurocognitive outcomes and functional magnetic resonance imaging networks using dual regression. Three main findings are reported: (i) large-scale network changes precede and follow interictal epileptiform discharges; (ii) the resilience of network topologies to interictal discharges is associated with stronger resting-state network connectivity; and (iii) vulnerability to interictal discharges is associated with worse neurocognitive outcomes. By combining the spatial resolution of functional magnetic resonance imaging with the temporal resolution of magnetoencephalography, we describe the effects of interictal epileptiform discharges on neurophysiological synchrony in intrinsic connectivity networks and establish the impact of interictal disruption of functional networks on cognitive outcome in children with epilepsy. The association between interictal discharges, network changes and neurocognitive outcomes suggests that it is of clinical importance to suppress discharges to foster more typical brain network development in children with focal epilepsy.

Keywords: functional connectivity; resting-state functional MRI; IED; graph theoretical analysis

Received April 23, 2014. Revised June 6, 2014. Accepted June 29, 2014. Advance Access publication August 7, 2014

Abbreviations: BOLD = blood oxygen level-dependent level; ICN = intrinsic connectivity network; IED = interictal epileptiform discharge

Introduction

The human brain exhibits exquisite hierarchical organization during rest, the maintenance of which consumes the majority of the brain's metabolic energy (Raichle and Mintun, 2006). The organization of functional brain activity at rest is readily measured using resting-state functional MRI, wherein brain regions that demonstrate covariance in spontaneous blood oxygen level-dependent level (BOLD) signal oscillations are said to form intrinsic connectivity network (ICNs; also known as resting-state networks) (Biswal *et al*., 1995; Raichle *et al*., 2001; Raichle and Snyder, 2007). Although these networks are conspicuous in infants (Fransson *et al*., 2007), with typical development, there are increases in the strength of long-range connections between brain regions associated within the same ICN, together with increasing segregation of cortical and subcortical structures associated with different ICNs (Dosenbach *et al*., 2010). These connectivity gradients reflect patterns of grey matter growth and subsequent synaptic pruning with age. Disruption of the organization of ICNs is an emerging area of interest in the study of neurodevelopmental conditions and has been proposed to impact childhood cognitive development (Uddin *et al*., 2013; Washington *et al*., 2014).

Children with epilepsy exhibit impairments in the development and segregation of these ICNs, which are related to the burden of the disease and neurocognitive function (Vaessen *et al*., 2013; Widjaja *et al*., 2013*a*, *b*; Ibrahim *et al*., 2014). Children who have abnormal EEGs with the presence of interictal spikes or sharp and/or slow waves also possess greater alterations in network organization than those who do not (Mankinen *et al*., 2012). The role of interictal epileptiform discharges (IEDs) is gaining greater prominence as a putative mechanism by which epilepsy interferes with normative organization of oscillatory brain networks, thereby leading to cognitive impairments (Gotman *et al*., 2005; Kobayashi *et al*., 2006; Fahoum *et al*., 2013). Disruption of ICNs has been associated with focal IEDs arising from multiple brain regions (Fahoum *et al*., 2013), highlighting the relevance of alterations of ICNs to the understanding of localization-related epilepsy. Furthermore, on a physiological level, the importance of IEDs is buttressed by observations that electric fields generated during these events are strong enough in intensity to influence action potential firing threshold and network synchronization (Grenier *et al*., 2003).

Understanding how IEDs interfere with ICNs and how these interactions relate to neurocognitive outcomes is important for several reasons. First, while the goal of medical and surgical treatments for epilepsy is to achieve seizure-freedom with minimal morbidity, the benefits of IED suppression are more controversial (Kuruvilla and Flink, 2003). Second, an understanding of the mechanisms of network impairments in this patient population may inform management strategies and the implementation of surgical treatments, including extent of resection of the irritative zone. Finally, while various authors have identified associations between disrupted ICNs and IEDs, the causal temporal relationships underlying these interactions have not been previously established.

Previous studies using BOLD-functional MRI have been limited by the fact that functional MRI indirectly measures neural activity, reflecting blood flow rather than direct neural processes. Moreover, BOLD dynamics are expressed on a slower timescale than are IEDs. Another modality that has been studied to characterize ICNs is MEG, which directly records neural oscillations and robustly reconstructs ICNs (de Pasquale *et al*., 2010, 2012; Brookes *et al*., 2011*a*, *b*). The superior temporal resolution of MEG has enabled mapping of oscillatory dynamics of ICN activity (de Pasquale *et al*., 2010, 2012) and may allow precise determination of how pathological processes affect ICNs without modelling these events using basis functions for haemodynamic responses. Furthermore, using MEG, oscillatory activity may also be analysed in physiologically-relevant frequency bands, an approach which has the potential to provide novel insights into the underlying neurophysiological processes involved in the development and disruption of ICNs.

In the present study, activity from brain regions comprising various ICNs were reconstructed from MEG recordings using resting-state functional MRI-informed coordinates to test the hypotheses that (i) IEDs are associated with changes in neurophysiological interactions within ICNs in children with focal epilepsy; (ii) that resilience and vulnerability of ICNs to such neurophysiological connectivity changes are associated with cognitive outcome; and (iii) ICN integrity as measured by functional MRI. A graph theoretical approach was applied to study changes in network topologies occurring in the peri-IED period on a millisecond timescale. The resilience or vulnerability of network topologies to change in this period was correlated with neurocognitive outcomes and functional MRI statistical parametric maps. Using a combined functional MRI-MEG approach, the current study provides evidence for disruption of neurophysiological connectivity in ICNs by IEDs, and uniquely demonstrates that such network alterations are associated with reduced ICN integrity and worse cognitive outcomes.

Materials and methods

Subject demographics

A total of 71 children with medically-intractable, focal (localization-related) epilepsy were recruited into this study from the Hospital for Sick Children in Toronto, Canada. Of these, 26 children were included in the current study. Children were excluded if (i) they required sedation; (ii) did not meet criteria for motion parameters for both functional MRI and MEG studies (as listed below); (iii) had a conspicuous MRI lesion that precluded accurate image registration; or (iv) if no

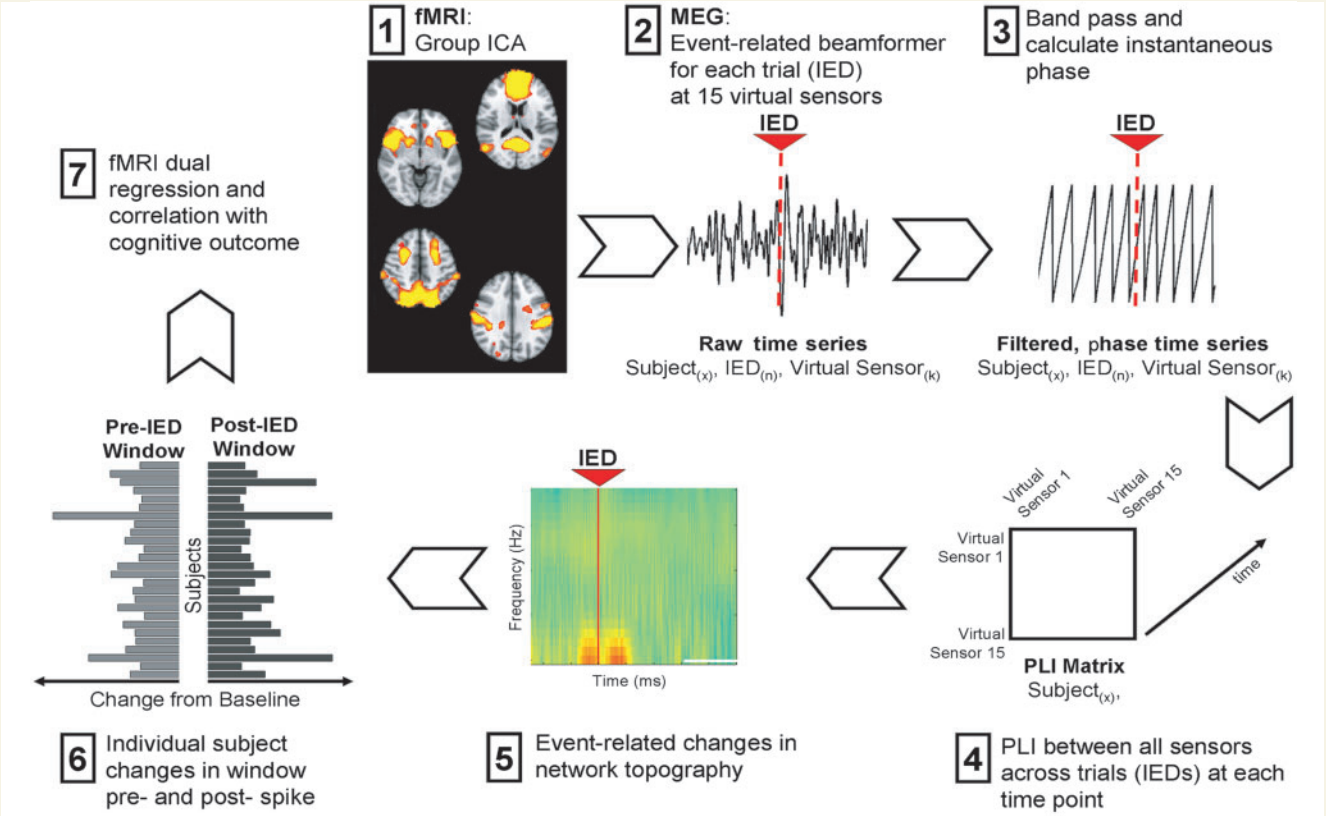

Figure 1 Analysis pipeline. (1) Temporally concatenated resting-state functional MRI data underwent group-independent component analysis to generate a group-average set of spatial maps. The MNI coordinates for the maxima of nodes of four ICNs were extracted. (2) The coordinates were then unwarped into the individual MEG headspace and oscillatory activity within these regions was reconstructed using a beamformer spatial filter. (3) The instantaneous phase of these oscillations was measured; and (4) phase-lag index was calculated for each sensor pair at each time point. (5) Network topologies were then measured using graph theory at each time point for each subject; and (6) variability ('resilience' and 'vulnerability') in the changes of network topology in a pre- and post-IED window were calculated. (7) The resilience of network topologies to IEDs was correlated with functional MRI statistical parametric maps using dual regression and to neurocognitive outcomes.

IEDs were captured on MEG. All patients underwent functional MRI and MEG studies without any sedation, which has been shown to alter BOLD signal and cortical oscillations (Marcar *et al*., 2006). Only one patient included had undergone a previous small cortical resection, which did not affect registration and the ICN networks were all adequately sampled. The children ranged in age from 7–17 years, with 13 (50%) males and with mean epilepsy duration (± standard deviation) of 4.56 ± 3.76 years. Nine children (35%) had epileptic foci localized to the temporal lobe, whereas 17 children (65%) had extra-temporal epilepsy and 15 children (58%) presented with secondarily generalized seizures (see Supplementary material for more details regarding subject demographics). The study complies with the Code of Ethics of the World Medical Association (Declaration of Helsinki) and was approved by the Research Ethics Board of the Hospital for Sick Children. Figure 1 shows a schematic of the processing pipeline used to combine functional MRI and MEG data, which are described in detail in subsequent sections.

Resting-state functional MRI processing

Structural and functional MRI data were collected using a 3 T scanner (Achieva magnet; Philips Healthcare) with an 8-channel phased array head coil. Patients were imaged using the epilepsy protocol, which included axial and coronal FLAIR (repetition time/echo time = 10 000/140 ms, section thickness = 3 mm, field of view = 22 cm, matrix = 316 × 290), axial and coronal T_2 and proton attenuation (repetition time/echo time = 4200/80/40 ms, section thickness = 3 mm, field of view = 22 cm, matrix = 400 × 272), volumetric 3D T_1 (repetition time/echo time = 4.9/2.3 ms, section thickness = 1 mm, field of view = 22 cm, matrix = 220 × 220), and resting state functional MRI (echo planar imaging, repetition time = 2000 ms, echo time = 30 ms, flip angle = 90°, matrix = 80 × 80 mm, voxel size = 2.875 × 2.875 × 4 mm, 180 volumes acquired and aligned to the anterior/posterior commissure line). Resting-state functional MRI was performed with the patient's eyes open while fixated on a cross presented via magnetic resonance-compatible goggles.

Preprocessing of resting-state data was performed using AFNI (http://afni.nimh.nih.gov/afni/) and FSL (http://fsl.fmrib.ox.ac.uk/fsl/fslwiki/). All subjects with a head displacement >2 mm in over two-thirds of the volumes collected or >2 mm overall were excluded from the analysis. The functional images were corrected for slice timing effects and were registered to the Montreal Neurological Institute (MNI152) 2 mm T_1 template via each subject's T_1-weighted structural image. The images were spatially smoothed using a 6.6 mm full-width

at half-maximum kernel. Preprocessed data were then bandpass filtered from 0.02 to 0.2 Hz. A general linear model was employed to regress the time course of CSF, white matter, global signal and six-parameter motion maximum displacement time courses from the data.

MEG acquisition and interictal epileptiform discharge marking

MEG data were acquired from the same cohort of children who were sleep-deprived the night before the acquisitions to accentuate focal IEDs. A whole-head gradiometer-based CTF/MISL Omega system (151 channels, VSM MedTech Ltd.) in a magnetically-shielded room was used. Fifteen 2-min periods of spontaneous data were recorded with simultaneous MEG and scalp EEG (International 10-20 system placement) with a sampling rate of 625 Hz, as previously published (Ochi *et al*., 2011). Data from 2-min segments with >5 mm head displacement between the beginning and end of the recording were discarded.

Interictal epileptiform discharges were identified based on the recommended International Federation of Clinical Neurophysiology recommendations: (i) sharp peak; (ii) duration between 20 and 200 ms; (iii) outstanding from ongoing background activity; and (iv) involvement of two or more MEG channels (Cobb, 1983). IEDs (spikes, polyspikes and sharp waves; median number: 82 events) were reviewed by clinical electrophysiologists from the 151-channel raw MEG waveforms with a bandpass filter of 1–70 Hz, which were cross-referenced to simultaneous EEG recordings. Spikes superimposed onto ECG tracings were excluded from the analysis. When polyspikes or repetitive spikes occur, the earliest spike peak with a reasonable magnetic field topography was selected (Ochi *et al*., 2011). This was performed because it has been previously shown that the zone of the earliest spike shows a high correlation with the seizure onset zone, defined by intracranial recordings (Hufnagel *et al*., 2000). The earliest peak of IEDs was marked as events for subsequent analysis.

Constructing intrinsic connectivity networks

To identify the coordinates of ICN nodes for MEG beamforming, an independent component analysis was first performed on temporally concatenated functional MRI data to generate a group-average set of spatial maps. This was achieved using the MELODIC toolbox in FSL. Four typical ICNs were extracted using group-independent component analysis, the default mode, salience, dorsal attention and motor networks (Fig. 2). The coordinates of the spatial maxima of the important nodes of these networks were then identified in standard MNI space and compared to coordinates described in the literature (Brier *et al*., 2012) (Table 1).

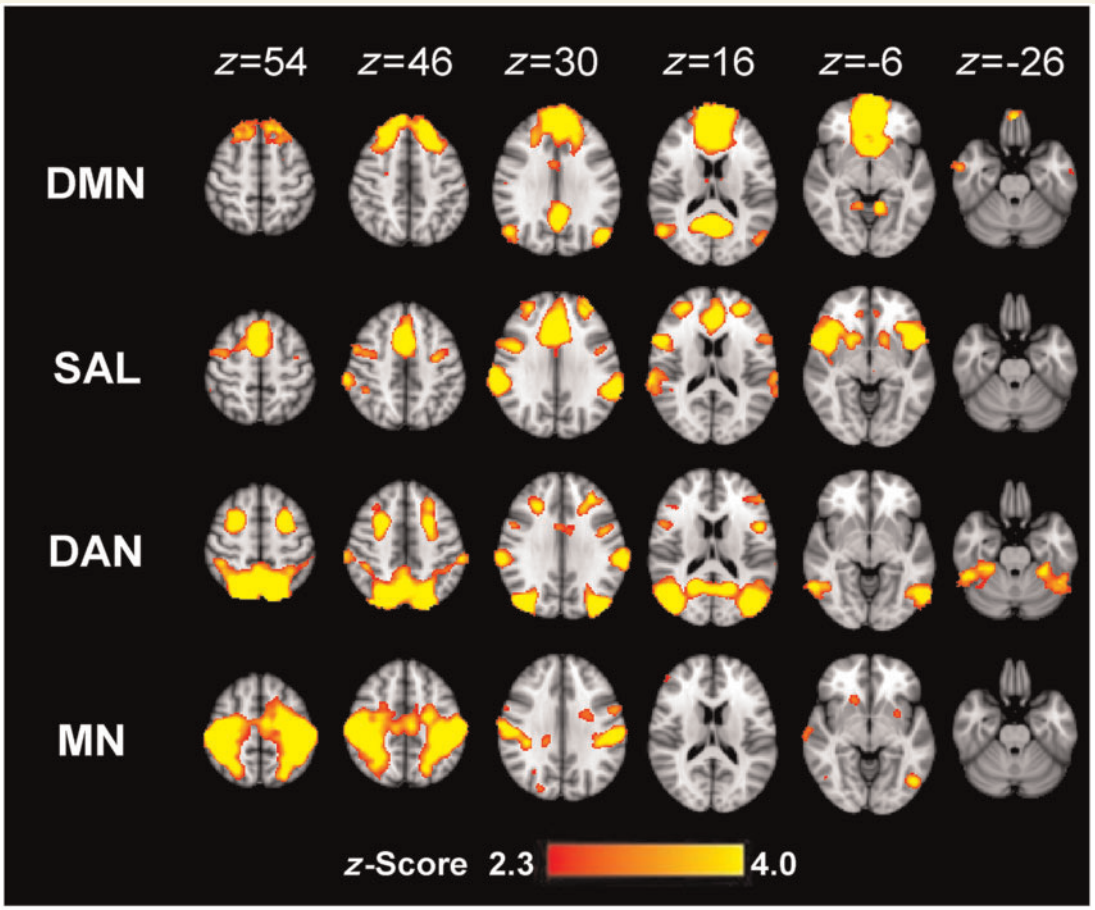

Figure 2 Group independent component analysis generates group-average set of spatial maps for four ICNs. Group-average spatial maps for the default mode network (DMN), salience network (SN), dorsal attention network (DAN) and motor network (MN) were calculated. The regional maxima corresponded closely to published data (Table 1).

Table 1 Spatial maxima of nodes of ICNs calculated using group independent component analysis in children with epilepsy and comparison with literature

Network	Node	Group independent component analysis coordinates (mm, MNI)			Literature coordinates (mm, MNI)		
		x	*y*	*z*	*x*	*y*	*z*
Default mode network	Posterior cingulate cortex	2	−60	22	0	−51	29
	Ventromedial prefrontal cortex	−2	52	−14	0	61	22
	Left lateral parietal	−50	−72	28	−48	−66	34
	Right lateral parietal	52	−68	22	53	−61	35
	Medial thalamus	−8	−8	14	0	−9	7
Salience network	Right insula	48	14	−8	43	7	2
	Left insula	−48	14	−6	−42	6	4
	Anterior cingulate cortex	2	20	34	12	32	30
Dorsal attention network	Left frontal eye fields	−24	2	56	−29	−5	55
	Right frontal eye fields	24	6	50	31	−5	54
	Left intraparietal sulcus	−64	−30	36	−45	−37	48
	Right intraparietal sulcus	66	−30	34	43	−36	46
Motor network	Right motor	42	−36	54	41	−22	48
	Left motor	−40	−38	52	−40	−23	53
	Supplementary motor area	−6	−16	50	1	−18	49

Literature coordinates from Brier *et al*. (2012).

Each subject's individual T_1 scan was registered to a standard MNI template using SPM2 (http://www.fil.ion.ucl.ac.uk/spm/). Additionally, multi-sphere headmodels were derived by fitting spheres (Lalancette *et al*., 2011) to each subject's inner-skull surface-derived via FSL. The coordinates of ICN nodes (15 in total) were then warped into individual headspaces of MEG acquisitions and broadband activity was reconstructed from each source location (2s before and 2s after each IED). A detailed explanation of the beamformer algorithms and constraints used is outlined in the Supplementary material. To ensure that the observed network changes were not attributable to leakage from strong sources occurring during IEDs, independent component analysis was also performed on the MEG data (Supplementary material) to remove components associated with the IEDs. Reproducible findings were shown from data rejecting high amplitude components attributable to IEDs. Furthermore, as will be discussed subsequently, oscillatory phase-locking was also quantified using the phase-lag index (Stam *et al*., 2007), which rejects zero-phase lag synchrony from common sources; therefore it is unlikely that the findings presented are attributable to signal leakage.

Spike-locked time-frequency analysis was performed on the reconstructed MEG data, as shown in the Supplementary material. The time–frequency plots were consistent to those previously reported in the literature using MEG (Bouet *et al*., 2012). The reconstructed data from each source were filtered into narrowband frequency ranges from 1–70 Hz with a bandwidth of 3 Hz FIR filters from the EEGLAB (eegfiltfft.m function) (Delorme and Makeig, 2004). The filtered signal was visually examined for edge and ringing artefacts. The instantaneous phase time series were then obtained for each source and frequency range using the band passed signal, $f(t)$, and its Hilbert transform, $\tilde{f}(t)$, as follows:

$$\varsigma(t) = f(t) + i\tilde{f}(t) = A(t)e^{i\phi(t)} \quad (1)$$

The Hilbert transform is related to the original signal by a $\frac{1}{2}\pi$ phase shift that does not alter the spectral distribution and is defined as:

$$HT(f(t)) = \tilde{f}(t) = \frac{1}{\pi} P.V. \int_{-\infty}^{\infty} \frac{f(t)}{t-\tau} d\tau \quad (2)$$

In this equation, P.V. denotes Cauchy principal value. From the original signal and its Hilbert transform, the instantaneous phase can be calculated as follows:

$$\theta(t) = \arctan\left(\frac{\tilde{f}(t)}{f(t)}\right) \quad (3)$$

The difference in the phase time series between any two nodes, j and k, $\Delta\theta_{j,k}(t)$, can be calculated and from the time series of the phase difference, the phase-lag index can be derived across trials as shown in Equation 4, where sgn denotes the sign or signum function. In the current analysis, phase analysis was performed across trials (IED events) at each time point. The phase-lag index has the distinct advantage of rejecting zero-phase lag synchrony, therefore mitigating interference from common sources, including signal leakage from the high amplitude components of IEDs.

$$PLI_{j,k,t} = \left| \frac{1}{N} \sum_{n=1}^{N} \mathrm{sgn}\left[\Delta\theta_{j,k}(t,n)\right] \right| \quad (4)$$

Network analysis in the peri-interictal epileptiform discharge period

Using the phase-lag index as an index of functional connectivity between each pair of sources, a 15 × 15 adjacency matrix was created for each subject at each time point in the peri-IED period by considering each IED as an individual trial. Network properties were measured by applying graph theoretical analysis using the Brain Connectivity Toolbox (Rubinov and Sporns, 2010). Two canonical measures of network topology were chosen for analysis: mean of clustering coefficient and characteristic path length. The mean clustering coefficient is measure of network segregation (Watts and Strogatz, 1998) or how the different ICN nodes tend to cluster together. Conversely, the characteristic path length is a measure of brain integration computed as the global average of the graph's distance matrix. A short path length suggests that each node can be reached from any other node along

a path composed of only a few edges. From these two measures, one is able to determine whether the network possesses a 'small-world' topology. This topology associated with efficient information transfer and is characteristic of many self-organized systems, including the human brain. Small-world networks possess a higher mean clustering coefficient and roughly equal path length compared to a random graph (Watts and Strogatz, 1998). The motivation for choosing these graph theoretical properties to analyse is that they represent fundamental summary measures of network topologies. Importantly, alterations in these measures has been previously reported in epileptic networks (Ibrahim *et al*., 2013) and in resting-state connectivity in patients with epilepsy (Wang *et al*., 2014).

To determine changes in network topologies occurring in the peri-IED epoch, a 500 ms baseline was chosen 1000 ms before the start of the IED. The choice of baseline was informed by the MEG literature (Bouet *et al*., 2012). To ensure that choice of baseline did not bias our findings, validations tests were performed with baselines of differing durations and latencies from IED onset (Supplementary material). A z-score of phase-lag index values at each analysed time point and 3 Hz frequency range, relative to baseline phase-lag index values in the same frequency range was derived to represent the change from this baseline in the peri-IED epoch. Children with network topologies that changed dramatically during this time period were defined as relatively 'vulnerable', whereas networks that did not exhibit large magnitudes of changes were termed relatively 'resilient' (Supplementary Fig. 4A). A discretized smoothing spline (based on the discrete cosine transform) was then applied to the data using the multidimensional robust automatic smoothing function, smoothn.m (Garcia, 2010).

Dual regression of functional MRI data

To test how resilience or vulnerability (i.e. the relative magnitude of change in network topologies between subjects) to IEDs influenced functional MRI statistical parametric maps, the set of spatial maps from the group-average analysis (which was used to establish coordinates for the important nodes of each network) was used to generate subject-specific versions of the spatial maps, and associated time series using dual regression (Filippini *et al*., 2009). First, for each subject, the group-average set of spatial maps were regressed (as spatial regressors in a multiple regression) into the subject's 4D space-time data set. This resulted in a set of subject-specific time series, one per group-level spatial map. Next those time series were regressed (as temporal regressors, again in a multiple regression) into the same 4D data set, resulting in a set of subject-specific spatial maps, one per group-level spatial map. We then used the indices of resilience and vulnerability of network topologies to IEDs as a regressor using FSL's Randomise permutation-testing tool (Nichols and Holmes, 2002). This algorithm shuffles the values of the covariate (networks susceptibility) between subjects 5000 times to assess how extreme the observed findings are from the random sampling distribution. Significance thresholds for cluster-based statistics were determined using 3dClustSim from the AFNI toolbox. This algorithm uses simulations to estimate the probability of a false positive (noise-only) cluster. It was determined that a cluster of 724 contiguous voxels was required for a corrected *P*-value of 0.05. This analysis approach allowed us to evaluate how changes in network topology in the peri-IED epoch, as determined by MEG are associated with ICN spatial maps, as measured by independent component analysis of functional MRI data.

Neuropsychological testing

Correlations between resilience and vulnerability of network topologies to IEDs and neuropsychological outcomes were also investigated. Both specific (functions attributable to the specific ICNs studied) and global functions were tested. Specific functions included working memory, which has been strongly associated with default mode network connectivity (Hampson *et al*., 2006; Yakushev *et al*., 2013); working memory was measured with forward and backward digit recall using the Digit Span subtest of the Wechsler Intelligence Scale for Children-IV (WISC-IV) (Wechsler, 2003). The full-scale IQ of the WISC-IV was correlated with neuroimaging data as a measure of global cognitive function (Wechsler, 2003). Age-adjusted z-scores were derived from raw scores (Ruff and Parker, 1993; Wechsler, 2003). Given the relatively small sample size of 26 children, any significant associations were subject to a test of robust fitness in MATLAB software. This algorithm uses iterative reweighted least squares with a bisquare weighting function to reject associations that are dominated by outliers.

Results

Changes in interictal epileptiform discharge-related network topology variably expressed across subjects

When event-related changes in network topology were calculated, it was found that both before and after IEDs, there was an increase in network clustering and a decrease in characteristic path length within the network formed by ICN nodes. The mean event-related network properties are shown in Fig. 3. These changes were most apparent in the 300 ms window before and after the IED.

The network changes associated with spikes both in the pre-IED and post-IED window were variably expressed between subjects. Individual subject changes in network topology in the pre- and post-IED intervals are shown in Fig. 3, along with the Bonferroni-corrected threshold for statistical significance. Subjects that expressed larger increases in mean network clustering in response to IEDs were considered more vulnerable to IEDs, whereas those who did not have large changes in network topology were considered resilient.

The resilience or vulnerability of ICNs was contrasted against clinical and demographic features of the children. There was no difference in changes in network topology in the pre- and post-IED window between children with temporal or extra-temporal lobe IEDs ($P = 0.61$ and $P = 0.88$, respectively), or between children with and without secondarily generalized seizures ($P = 0.31$ and $P = 0.65$, respectively) and no significant association was identified with child age ($P = 0.35$ and $P = 0.16$, respectively) and epilepsy duration ($P = 0.75$ and $P = 0.49$, respectively).

Changes in graph properties of individual network nodes were calculated to assess whether the involvement of more nodes was related to greater changes in network topology in the peri-IED period (Supplementary material). There was a significant association between the number of nodes affected and network vulnerability in the post-spike ($P < 0.001$) but not pre-spike ($P = 0.12$)

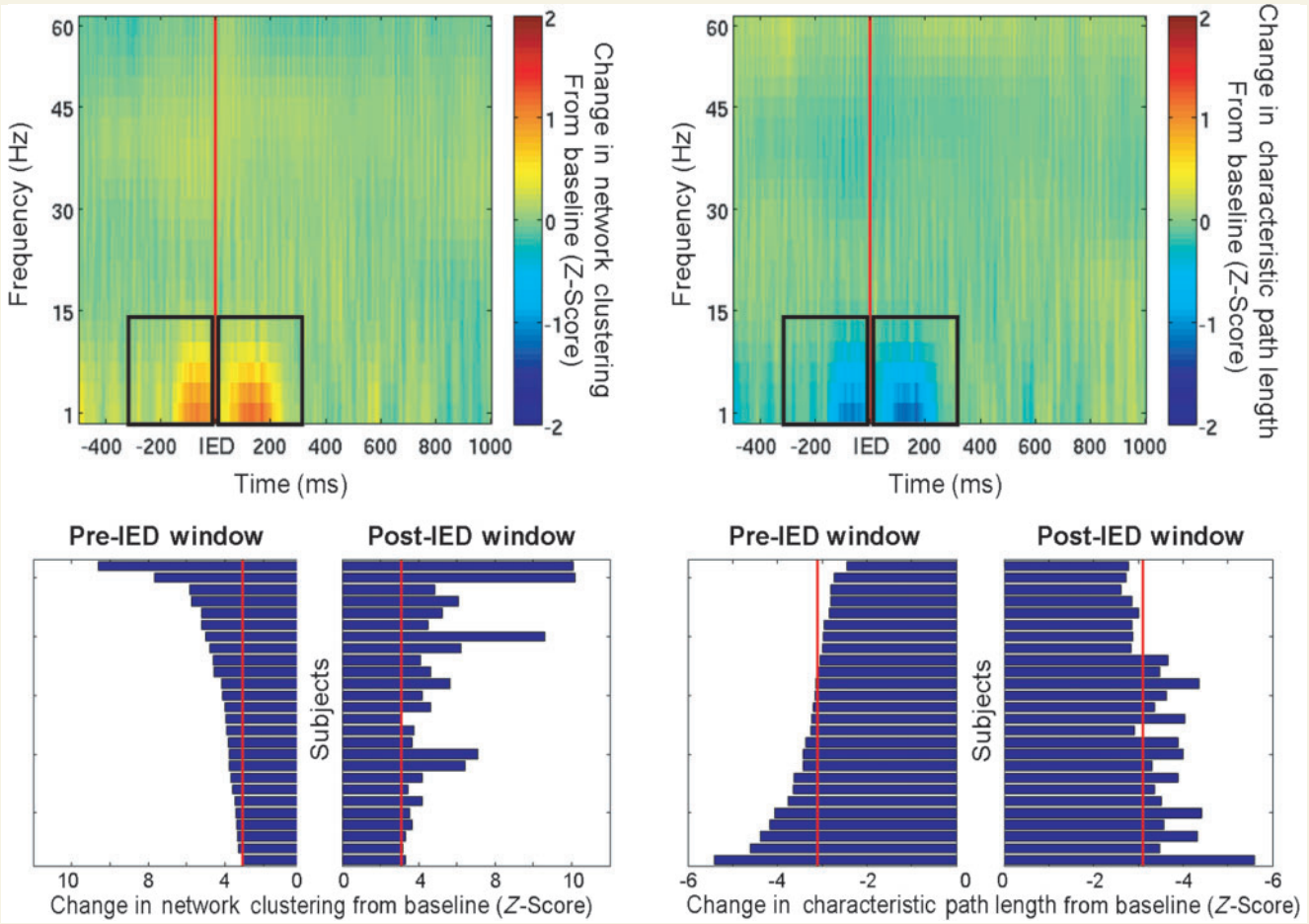

Figure 3 IED-locked changes in network topology. *Top*: Average event-related network changes for all subjects showing an increase in mean network clustering and a decrease in characteristic path length both preceding and following IEDs, suggesting a shift away from a small-world network. Black boxes represent pre- and post-IED windows. *Bottom*: Changes in network topology within pre- and post-IED windows amongst all subjects. Greater changes reflect more vulnerable topologies, whereas smaller changes reflect resilience. Red line denotes Bonferroni-corrected threshold ($P < 0.05$; corrected across subjects) for significant changes from baseline within defined interval.

period, implying that pre-spike changes in connectivity are network specific whereas post-spike changes are a larger network phenomenon.

A significant relationship was identified between changes in network topology in both the pre- and post-IED window and the frequency of IEDs ($R = 0.57$, $P < 0.01$ and $R = 0.67$, $P < 0.01$). While subjects that had higher IED numbers had greater changes in network topologies, these changes could not be exclusively attributed to the fact that a greater number of events (IEDs) were analysed. As presented in the Supplementary material, the magnitude of the network changes in the peri-IED period was not diminished by analysing only a subset of the recorded IEDs from these patients.

Resilience to interictal epileptiform discharges associated with integrity of intrinsic connectivity networks

Resilience, the measure of relative change in network topology from baseline in the pre- and post-IED intervals was regressed against the functional MRI data. Dual regression was used to determine how ICNs are related to resilience or vulnerability of network topologies to IEDs. As shown in Fig. 4 and summarized in Tables 2 and 3, network topologies that were resilient to IEDs measured using MEG were associated with stronger ICN connectivity as indexed by resting-state functional MRI. Conversely, network topologies that were vulnerable to IEDs were associated with weaker ICNs and greater inter-network functional connectivity.

Children with greater resilience to IED-related changes showed significantly stronger contributions of the posterior cingulate cortex/precuneus, ventromedial prefrontal cortex and anterior cingulate cortex to the default mode network independent component analysis map; whereas those who were more vulnerable had significantly stronger contributions from regions not associated with the default mode network (intraparietal sulcus, ventral anterior cingulate cortex), implying a less robustly segregated network. Similarly, the independent components of the salience network, dorsal attention network and motor network had greater contributions from regions associated with those networks and less

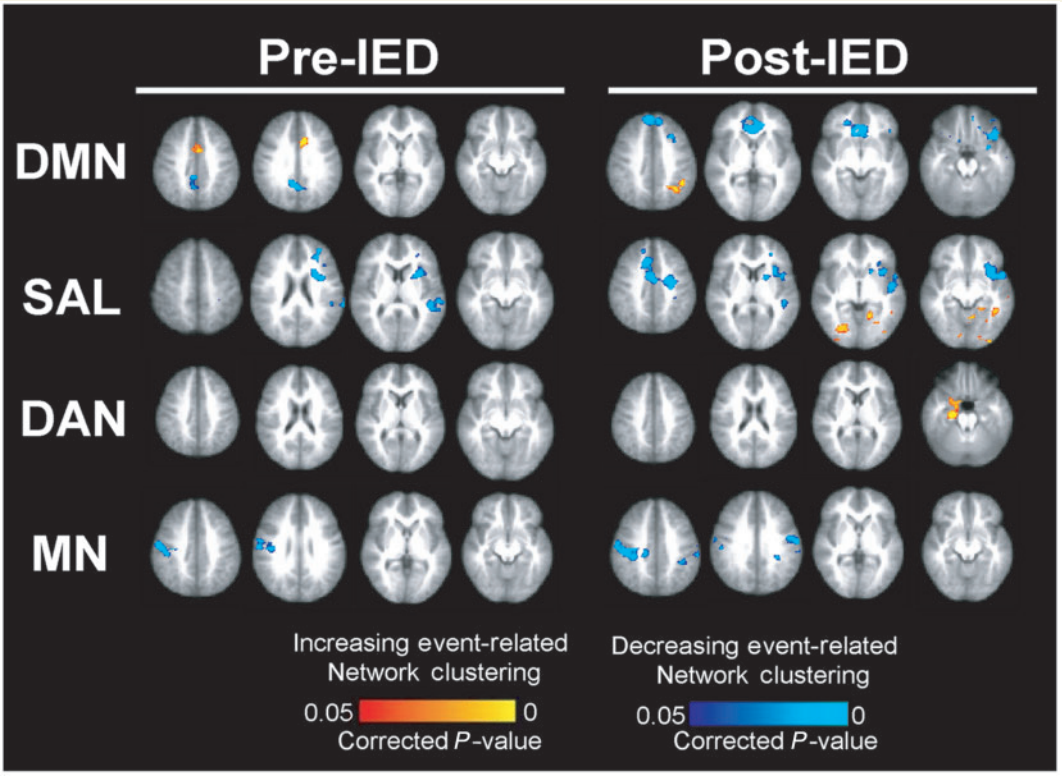

Figure 4 Association between resilience to IEDs and functional MRI statistical parametric maps. Dual regression of independent component analysis maps showed that patients with network topologies that were more resilient to IEDs showed stronger connectivity within ICNs. Those with greater vulnerability to IEDs had weaker connectivity within network components and greater connectivity between different networks.

Table 2 Differences in network components associated pre-IED network clustering

Contrast	Network	Region	1 − *P*-value	Cluster size	MNI coordinates (mm)		
Resilient topology (less change in pre-IED network topology)							
	Default mode network	Posterior cingulate cortex/precuneus	0.999	797	8	−50	32
	Salience network	Left superior temporal gyrus	0.999	1469	−66	−32	12
		Left insula	0.999	903	−36	16	4
	Motor network	Right rolandic	0.999	853	42	−16	32
Vulnerable topology (greater change in pre-IED network topology)							
	Default mode network	Ventral anterior cingulate cortex	0.999	1297	−8	16	34

contribution from external cortical areas in children with more resilient network topologies.

Intrinsic connectivity network resilience to interictal epileptiform discharges is associated with improved cognitive outcome

When neurophysiological data were compared to neuropsychological data, it was found that networks with topologies that were more vulnerable to changes post-IED (with greater magnitude of change in network clustering coefficient following an IED) were associated with lower full-scale IQ scores ($R = -0.49$; $P = 0.017$). When subjects with fewer than 50 recorded IEDs (six subjects) were excluded from the analysis, as these individuals may introduce noise into the phase-locking measurements, the inverse relationship between network vulnerability to IEDs and full-scale IQ became stronger ($R = -0.64$; $P < 0.01$). Changes in network topologies prior to the IED also showed a strong trend towards association with full-scale IQ ($R = -0.39$, $P = 0.06$). There was no association between altered network topology and other domain-specific neuropsychological measures.

Because subjects who were more prone to a higher frequency of IEDs (as indexed by the number of IEDs captured during the fixed duration of the recordings) were more likely to have lower

Table 3 Differences in network components associated post-IED network clustering

Contrast	Network	Region	1 – *P*-value	Cluster size	MNI coordinates (mm)		
Resilient topology (less change in pre-IED network topology)							
	Default mode network	Left inferior frontal gyrus	0.999	2103	−34	22	−20
		Ventromedial prefrontal cortex	0.999	1089	0	52	32
		ACC	0.999	810	4	24	16
	Salience network	Left insula	0.999	2082	−30	18	−12
		Ventral anterior cingulate cortex	0.999	1830	10	20	24
		Left superior temporal gyrus	0.999	1437	−48	−36	14
	Motor network	Left rolandic	0.999	1652	−60	−16	38
		Right rolandic	0.999	1510	44	−26	42
Vulnerable topology (greater change in pre-IED network topology)							
	Default mode network	Right intraparietal sulcus	0.999	1178	−32	−52	34
	Salience network	Occipital cortex	0.999	2552	−30	−32	−24
	Dorsal attention network	Right hippocampus	0.999	902	28	−20	−22

IQ scores (Pearson correlation: −0.47; $P = 0.02$), we tested the independent associations between number of IEDs captured, network susceptibility and IQ (Supplementary material). Network resilience/vulnerability uniquely accounted for nearly twice the variance in IQ compared to number of IEDs captured (0.062 versus 0.032). Furthermore, in a multivariate stepwise regression, the number of IEDs captured was rejected ($P = 0.36$) and network susceptibility was included in the final model ($P = 0.01$). Children with less resilient networks were found to be prone to a greater frequency of IEDs, and we also found that the combined contribution of network changes and IEDs is strongly associated with IQ (see principal component analysis in the Supplementary material).

Discussion

Using a combined functional MRI-MEG approach, the current study provides a unique investigation of alterations of neurophysiological interactions in ICNs during IEDs. Three main findings are reported. First, large-scale network changes both preceded and followed IEDs implying that reorganization in the influence of the larger embedded network may play a causal role in the expression of IEDs. Second, the resilience of network topologies to IEDs was associated with stronger ICNs; and third, vulnerability to IEDs was associated with worse neurocognitive outcomes. These findings add substantially to previously identified associations between IEDs, ICNs and neurocognitive outcomes.

Large-scale network changes precede interictal epileptiform discharges

The finding that large-scale network changes are not only associated with IEDs, but are present before their onset provides novel insight into the relationship between epileptogenic events and brain oscillations and suggests that oscillatory interactions in distributed brain networks may be involved in the initiation of IEDs. The view that reorganized large-scale networks may play a causal role in the release of IEDs is supported by evidence showing that epileptogenic brain regions often become functionally disconnected minutes to hours before ictal events. During the preictal period, when IEDs become particularly accentuated, epileptogenic areas demonstrate decreased interactions with surrounding cortex, as indexed by reduced inter-regional phase synchrony (Le Van Quyen *et al*., 2001; Ibrahim *et al*., 2013). Moreover, Kramer *et al*. (2010) determined that seizure onset is characterized by a global breakdown in inter-regional coupling across the cerebral cortex with altered network topologies.

Desynchronizations may functionally isolate the epileptogenic regions from the influence of large-scale brain networks, creating an idle population of neurons that may be more susceptible to recruitment into seizure. Such desynchronizations may also represent depression of synaptic inhibition in areas around epileptogenic cortex, isolating it from the controlling influence of the embedded network (Uhlhaas and Singer, 2006). Here, we show that large-scale network changes also precede IEDs, supporting the view that epileptic dynamics cannot be viewed in isolation, but rather should be understood in the context of a dynamic system of inter-regional communication within a larger network.

Our findings are also concordant with prior reports of BOLD signal changes on functional MRI that precede IED expression. Makiranta *et al*. (2005) showed that BOLD changes precede IEDs after penicillin injection in pig models, and Diehl *et al*. (1998) identified changes in middle cerebral artery flow before generalized spike and wave discharges. BOLD changes were also recently identified preceding IEDs in patients with generalized (Moeller *et al*., 2008) and focal (Jacobs *et al*., 2009) epilepsy syndromes. The current report presents the first evidence of altered neural synchrony within ICNs using direct measurement of neural activity using MEG. In addition to the superior temporal resolution afforded by MEG, this approach circumvents the challenge of modelling neural events with haemodynamic response basis functions, which may be unpredictably variable in this circumstance (Jacobs *et al*., 2008). In concordance with other studies, these findings were generalizable across different underlying epileptogenic syndromes (Jacobs *et al*., 2009) and locations of seizure foci (Fahoum *et al*., 2013). The finding that network

changes were not present specifically at the time of the IED may reflect a rejection of zero-phase lag synchrony by the phase-lag index, given the high amplitude increase in neuromagnetic signal during IEDs.

Interictal epileptiform discharges, intrinsic connectivity networks and neurocognitive outcome

It has long been suspected that IEDs may contribute to impaired neurocognitive function in patients with epilepsy and the interaction between IEDs and cognitively-salient oscillatory networks is an area of increasing scientific inquiry. Previous studies have reported spike-related BOLD decreases in default mode network regions (Kobayashi *et al*., 2006; Laufs *et al*., 2007). Such IED-associated deactivations accompany spikes of differing morphologies and locations, including generalized spike and wave discharges or focal interictal discharges of temporal, frontal and posterior quadrant origins (Fahoum *et al*., 2012, 2013). In patients with idiopathic generalized epilepsy, thalamocortical activation and suspension of regions of the default mode network were hypothesized to contribute to reduced responsiveness during IEDs (Gotman *et al*., 2005).

An understanding of the associations between IEDs, oscillatory brain networks and cognition is critical to devise appropriate treatment strategies aimed at improving outcomes in this patient population. In the current report, changes in ICN topologies, particularly following IEDs, were significantly associated with functional MRI statistical parametric maps of networks and neurocognitive outcomes. The segregation of ICNs is a hallmark of typical development (Dosenbach *et al*., 2010). Connectivity gradients between task-positive and task-negative ICN hubs become stronger during adolescence and early adulthood with sharpening of the boundaries of the default mode network and decreased correlation between the default mode and attention control networks (Anderson *et al*., 2011). The fractionation of brain regions into specific regional hubs also represents a transition from a local to distributed network organization, which characterizes typical childhood and adolescent development (Fair *et al*., 2009). This intra-network integration and inter-network segregation contributes to the emergence of the more mature distributed, functionally-specialized networks observed in adults.

The disruption of normative ICN organization in children with network topologies that were vulnerable to IEDs provides novel insights into the interactions between epileptic dynamics, oscillatory synchrony and the organization of spontaneous network connectivity in the developing brain. It was observed that the physiological anti-correlation between task-positive networks (salience network, dorsal attention network, motor network) and a task-negative network (default mode network) was weaker in children with greater vulnerability to IEDs. The loss of these connectivity gradients has also been previously associated with worse neurocognitive outcomes in a similar set of children with epilepsy when compared with age-matched controls (Ibrahim *et al*., 2014). Since the majority of resting-state studies do not differentiate between baseline periods that are and are not IED-free, this study underscores the importance of evaluating IEDs when studying oscillatory networks in patients with epilepsy. We also provide evidence supporting more aggressive suppression of discharges through medical or surgical treatments, as these results indicate that IEDs are not benign in regards to neurocognitive development.

Neuromagnetic oscillations, BOLD intrinsic connectivity networks and frequency specificity

Neuromagnetic recordings were used to reconstruct oscillatory activity from coordinates of ICN nodes, identified using functional MRI. This approach capitalizes on recent advances in the use of MEG for investigating neurophysiological oscillations in ICNs, which are most accurately localized using functional MRI guidance. ICNs have been previously reconstructed from band-limited power (BLP; the power of envelope modulation of a relatively narrow range of frequencies) correlations among MEG signals reconstructed from various locations in the brain. BLP was shown to demonstrate significant interhemispheric correlations between homologous brain regions, as would be expected from spontaneous fluctuations in BOLD signal across multiple frequencies (Liu *et al*., 2010). Furthermore, source space localization in MEG demonstrates long-range temporal correlation between spontaneous BLP signals from functionally-related regions (Brookes *et al*., 2011*b*; Hipp *et al*., 2012). Correlations of BLP within ICNs were strongest in these studies in the alpha and beta frequency ranges, depending on the underlying oscillation frequency. Furthermore, the spatial structure of several canonical ICNs have been reconstructed from MEG (de Pasquale *et al*., 2010, 2012; Brookes *et al*., 2011*a*). These studies again demonstrated that ICNs are best captured by fluctuations in theta, alpha and beta oscillations.

An important advantage of measuring ICNs using MEG is the ability to analyse changes in network topologies in physiologically-relevant frequency bands. In the current study, we found that the strongest changes in network topology, both before and after IEDs occurred in lower frequency bands (namely, delta and theta). This is supported by previous findings that IEDs with slow waves on EEG were more likely to cause default mode network deactivation than those lacking slow waves (Kobayashi *et al*., 2006). Recently, data from combined functional MRI-intracranial EEG revealed that runs of IEDs and short electroencephalographic seizures were associated with decreased gamma power and increases in the power of lower frequency oscillations, although the findings were inconsistently expressed across the six subjects studied (Fahoum *et al*., 2013). Although our study differed considerably in methodology and techniques, time-frequency analysis also revealed increases in the power of lower frequencies along with some decreases in gamma power, although as Fahoum *et al.* (2013) report, the latter were greatly exceeded by the former. Finally, power increases in slower oscillations in ICNs nodes has been previously linked to consciousness. For instance, Blumenfeld *et al.* (2004) found that increased delta frequency power in the default mode network, linked to impaired

consciousness in patients with complex partial seizures with intracranial electrodes (Englot *et al*., 2010).

Limitations and future directions

An important question is why some brains are more resilient, while others more vulnerable to changes in network topology in the peri-IED epoch. Using recent functional neuroimaging methods, neuroscientists are able to improve classification of illness and stratify patient populations based on specific resting- or event-related network impairments, as performed in the current study. Patients who are prone to having more frequent IEDs demonstrate greater vulnerability to changes in network topology. We have shown, however, that this increased vulnerability cannot be attributed to the greater number of IEDs analysed and explains more of the variance in neurocognitive outcome than the number of IEDs captured during the recording (Supplementary material). The findings imply that the oscillatory organization of brain networks in children who are more prone to IEDs is intrinsically less resilient than those with fewer events. It is possible that the vulnerability may be mediated by dysfunctional cortical or subcortical circuitry in children who are more prone to having frequent IEDs. Notably, the thalamus may play an important role in mediating oscillatory network resilience as well as the expression of IEDs. We have previously shown that more severe epilepsy syndromes are characterized by a loss of centrality of the thalamus in a whole-brain connectome (Ibrahim *et al*., 2014). It has also been shown that synchronous spike-and-wave discharges reflect highly synchronized oscillations in thalamocortical networks, although spike and wave discharges originate in the cortex and initiate oscillations in the thalamo-cortical-thalamic loop (Meeren *et al*., 2002). Multimodality studies evaluating effective connectivity or causal directed information flow are needed to disentangle these effects and explain variability in resilience of oscillatory neural networks.

The primary limitation of the current study is the heterogeneity in clinical syndromes of children with epilepsy, including the location of seizure foci, epileptogenic substrates and antiepileptic medications. Previous studies have, however, suggested that large-scale network changes in the peri-IED period are generalizable across different patient groups and, indeed, we found no significant difference in resilience or vulnerability to IEDs across different clinical variables. Furthermore, it is expected that if variability in the clinical population impacts the measured network topologies, it would have an effect of diminishing the observed findings. Another limitation is the visual marking of IEDs, where imprecision in marking may introduce greater bias in the identification of altered connectivity at higher frequencies. Future studies with larger patient cohorts are indicated to better characterize the heterogeneity and to correlate them to specific network impairments.

Conclusion

Using a novel combined functional MRI-MEG approach, the current study examined neurophysiological changes in ICN topologies in the peri-IED epoch and correlated the resilience and vulnerability to network changes with neurocognitive function in children. It was found that changes in the topology of ICNs both preceded and followed the IEDs. The resilience of ICNs to changes in the peri-IED epoch, as measured by MEG was associated with greater segregation of these networks on functional MRI as well as improved neurocognitive outcomes in affected children. The association between IEDs, network changes and neurocognitive outcomes highlights their importance in understanding and treating the comorbidities of intractable childhood epilepsy.

Funding

This research was supported by the Canadian Institutes of Health Research (CIHR) Vanier Canada Graduate Scholarship, CIHR Bisby Fellowship, The Hospital for Sick Children Foundation Student Scholarship Program, The Hospital for Sick Children Centre for Brain and Behaviour, the Ontario Brain Institute, the Wiley Family and Jack Beqaj Funds for Epilepsy Surgery Research, and the University of Toronto Surgeon-Scientist Program.

Supplementary material

Supplementary material is available at *Brain* online.

References

Anderson JS, Ferguson MA, Lopez-Larson M, Yurgelun-Todd D. Connectivity gradients between the default mode and attention control networks. Brain Connect 2011; 1: 147–57.

Biswal B, Yetkin FZ, Haughton VM, Hyde JS. Functional connectivity in the motor cortex of resting human brain using echo-planar MRI. Magn Reson Med 1995; 34: 537–41.

Blumenfeld H, Rivera M, McNally KA, Davis K, Spencer DD, Spencer SS. Ictal neocortical slowing in temporal lobe epilepsy. Neurology 2004; 63: 1015–21.

Bouet R, Jung J, Delpuech C, Ryvlin P, Isnard J, Guenot M, et al. Towards source volume estimation of interictal spikes in focal epilepsy using magnetoencephalography. Neuroimage 2012; 59: 3955–66.

Brier MR, Thomas JB, Snyder AZ, Benzinger TL, Zhang D, Raichle ME, et al. Loss of intranetwork and internetwork resting state functional connections with Alzheimer's disease progression. J Neurosci 2012; 32: 8890–9.

Brookes MJ, Hale JR, Zumer JM, Stevenson CM, Francis ST, Barnes GR, et al. Measuring functional connectivity using MEG: methodology and comparison with fcMRI. Neuroimage 2011a; 56: 1082–104.

Brookes MJ, Woolrich M, Luckhoo H, Price D, Hale JR, Stephenson MC, et al. Investigating the electrophysiological basis of resting state networks using magnetoencephalography. Proc Natl Acad Sci USA 2011b; 108: 16783–8.

Cobb WA. Recommendations for the practice of clinical neurophysiology. Amsterdam: Elsevier; 1983.

de Pasquale F, Della Penna S, Snyder AZ, Lewis C, Mantini D, Marzetti L, et al. Temporal dynamics of spontaneous MEG activity in brain networks. Proc Natl Acad Sci USA 2010; 107: 6040–5.

de Pasquale F, Della Penna S, Snyder AZ, Marzetti L, Pizzella V, Romani GL, et al. A cortical core for dynamic integration of functional networks in the resting human brain. Neuron 2012; 74: 753–64.

Delorme A, Makeig S. EEGLAB: an open source toolbox for analysis of single-trial EEG dynamics including independent component analysis. J Neurosci Methods 2004; 134: 9–21.

Diehl B, Knecht S, Deppe M, Young C, Stodieck SR. Cerebral hemodynamic response to generalized spike-wave discharges. Epilepsia 1998; 39: 1284–9.

Dosenbach NU, Nardos B, Cohen AL, Fair DA, Power JD, Church JA, et al. Prediction of individual brain maturity using fMRI. Science 2010; 329: 1358–61.

Englot DJ, Yang L, Hamid H, Danielson N, Bai X, Marfeo A, et al. Impaired consciousness in temporal lobe seizures: Role of cortical slow activity. Brain 2010; 133: 3764–77.

Fahoum F, Zelmann R, Tyvaert L, Dubeau F, Gotman J. Epileptic discharges affect the default mode network–FMRI and intracerebral EEG evidence. PLoS One 2013; 8: e68038.

Fahoum F, Lopes R, Pittau F, Dubeau F, Gotman J. Widespread epileptic networks in focal epilepsies: EEG-fMRI study. Epilepsia 2012; 53: 1618–27.

Fair DA, Cohen AL, Power JD, Dosenbach NU, Church JA, Miezin FM, et al. Functional brain networks develop from a "local to distributed" organization. PLoS Comput Biol 2009; 5: e1000381.

Filippini N, MacIntosh BJ, Hough MG, Goodwin GM, Frisoni GB, Smith SM, et al. Distinct patterns of brain activity in young carriers of the APOE-epsilon4 allele. Proc Natl Acad Sci USA 2009; 106: 7209–14.

Fransson P, Skiold B, Horsch S, Nordell A, Blennow M, Lagercrantz H, et al. Resting-state networks in the infant brain. Proc Natl Acad Sci USA 2007; 104: 15531–6.

Garcia D. Robust smoothing of gridded data in one and higher dimensions with missing values. Comput Stat Data Anal 2010; 54: 1167–78.

Gotman J, Grova C, Bagshaw A, Kobayashi E, Aghakhani Y, Dubeau F. Generalized epileptic discharges show thalamocortical activation and suspension of the default state of the brain. Proc Natl Acad Sci USA 2005; 102: 15236–40.

Grenier F, Timofeev I, Crochet S, Steriade M. Spontaneous field potentials influence the activity of neocortical neurons during paroxysmal activities in vivo. Neuroscience 2003; 119: 277–91.

Hampson M, Driesen NR, Skudlarski P, Gore JC, Constable RT. Brain connectivity related to working memory performance. J Neurosci 2006; 26: 13338–43.

Hipp JF, Hawellek DJ, Corbetta M, Siegel M, Engel AK. Large-scale cortical correlation structure of spontaneous oscillatory activity. Nat Neurosci 2012; 15: 884–90.

Hufnagel A, Dumpelmann M, Zentner J, Schijns O, Elger CE. Clinical relevance of quantified intracranial interictal spike activity in presurgical evaluation of epilepsy. Epilepsia 2000; 41: 467–78.

Ibrahim GM, Anderson R, Akiyama T, Ochi A, Otsubo H, Singh-Cadieux G, et al. Neocortical pathological high frequency oscillations are associated with frequency-dependent alterations in functional network topology. J Neurophysiol 2013; 110: 2475–83.

Ibrahim GM, Morgan BR, Lee W, Smith ML, Donner EJ, Wang F, et al. Impaired development of intrinsic connectivity networks in children with medically intractable localization-related epilepsy. Hum Brain Mapp 2014 [Epub ahead of print].

Jacobs J, Hawco C, Kobayashi E, Boor R, LeVan P, Stephani U, et al. Variability of the hemodynamic response as a function of age and frequency of epileptic discharge in children with epilepsy. Neuroimage 2008; 40: 601–14.

Jacobs J, Levan P, Moeller F, Boor R, Stephani U, Gotman J, et al. Hemodynamic changes preceding the interictal EEG spike in patients with focal epilepsy investigated using simultaneous EEG-fMRI. Neuroimage 2009; 45: 1220–31.

Kobayashi E, Bagshaw AP, Benar CG, Aghakhani Y, Andermann F, Dubeau F, et al. Temporal and extratemporal BOLD responses to temporal lobe interictal spikes. Epilepsia 2006; 47: 343–54.

Kramer MA, Eden UT, Kolaczyk ED, Zepeda R, Eskandar EN, Cash SS. Coalescence and fragmentation of cortical networks during focal seizures. J Neurosci 2010; 30: 10076–85.

Kuruvilla A, Flink R. Intraoperative electrocorticography in epilepsy surgery: useful or not? Seizure 2003; 12: 577–84.

Lalancette M, Quraan M, Cheyne D. Evaluation of multiple-sphere head models for MEG source localization. Phys Med Biol 2011; 56: 5621–35.

Laufs H, Hamandi K, Salek-Haddadi A, Kleinschmidt AK, Duncan JS, Lemieux L. Temporal lobe interictal epileptic discharges affect cerebral activity in "default mode" brain regions. Hum Brain Mapp 2007; 28: 1023–32.

Le Van Quyen M, Martinerie J, Navarro V, Baulac And M, Varela FJ. Characterizing neurodynamic changes before seizures. J Clin Neurophysiol 2001; 18: 191–208.

Liu Z, Fukunaga M, de Zwart JA, Duyn JH. Large-scale spontaneous fluctuations and correlations in brain electrical activity observed with magnetoencephalography. Neuroimage 2010; 51: 102–11.

Makiranta M, Ruohonen J, Suominen K, Niinimaki J, Sonkajarvi E, Kiviniemi V, et al. BOLD signal increase preceeds EEG spike activity–a dynamic penicillin induced focal epilepsy in deep anesthesia. Neuroimage 2005; 27: 715–24.

Mankinen K, Jalovaara P, Paakki JJ, Harila M, Rytky S, Tervonen O, et al. Connectivity disruptions in resting-state functional brain networks in children with temporal lobe epilepsy. Epilepsy Res 2012; 100: 168–78.

Marcar VL, Schwarz U, Martin E, Loenneker T. How depth of anesthesia influences the blood oxygenation level-dependent signal from the visual cortex of children. AJNR Am J Neuroradiol 2006; 27: 799–805.

Meeren HK, Pijn JP, Van Luijtelaar EL, Coenen AM, Lopes da Silva FH. Cortical focus drives widespread corticothalamic networks during spontaneous absence seizures in rats. J Neurosci 2002; 22: 1480–95.

Moeller F, Siebner HR, Wolff S, Muhle H, Boor R, Granert O, et al. Changes in activity of striato-thalamo-cortical network precede generalized spike wave discharges. Neuroimage 2008; 39: 1839–49.

Nichols TE, Holmes AP. Nonparametric permutation tests for functional neuroimaging: a primer with examples. Hum Brain Mapp 2002; 15: 1–25.

Ochi A, Go CY, Otsubo H. Clinical MEG analyses for children with intractable epilepsy. In: Pang E, editor. Magneoencephalography. Rijeka: InTech; 2011.

Raichle ME, Mintun MA. Brain work and brain imaging. Annu Rev Neurosci 2006; 29: 449–76.

Raichle ME, Snyder AZ. A default mode of brain function: a brief history of an evolving idea. Neuroimage 2007; 37: 1083–90; discussion 1097–9.

Raichle ME, MacLeod AM, Snyder AZ, Powers WJ, Gusnard DA, Shulman GL. A default mode of brain function. Proc Natl Acad Sci USA 2001; 98: 676–82.

Rubinov M, Sporns O. Complex network measures of brain connectivity: uses and interpretations. Neuroimage 2010; 52: 1059–69.

Ruff RM, Parker SB. Gender- and age-specific changes in motor speed and eye-hand coordination in adults: normative values for the finger tapping and grooved pegboard tests. Percept Mot Skills 1993; 76: 1219–30.

Stam CJ, Nolte G, Daffertshofer A. Phase lag index: assessment of functional connectivity from multi channel EEG and MEG with diminished bias from common sources. Hum Brain Mapp 2007; 28: 1178–93.

Uddin LQ, Supekar K, Lynch CJ, Khouzam A, Phillips J, Feinstein C, et al. Salience network-based classification and prediction of symptom severity in children with autism. JAMA Psychiatry 2013; 70: 869–79.

Uhlhaas PJ, Singer W. Neural synchrony in brain disorders: relevance for cognitive dysfunctions and pathophysiology. Neuron 2006; 52: 155–68.

Vaessen MJ, Braakman HM, Heerink JS, Jansen JF, Debeij-van Hall MH, Hofman PA, et al. Abnormal modular organization of functional networks in cognitively impaired children with frontal lobe epilepsy. Cereb Cortex 2013; 23: 1997–2006.

Wang J, Qiu S, Xu Y, Liu Z, Wen X, Hu X, et al. Graph theoretical analysis reveals disrupted topological properties of whole brain functional networks in temporal lobe epilepsy. Clin Neurophysiol 2014.

Washington SD, Gordon EM, Brar J, Warburton S, Sawyer AT, Wolfe A, et al. Dysmaturation of the default mode network in autism. Hum Brain Mapp 2014; 35: 1284–96.

Watts DJ, Strogatz SH. Collective dynamics of 'small-world' networks. Nature 1998; 393: 440–2.

Wechsler D. WISC-IV administration manual. San Antonio, TX: The Psychological Corporation; 2003.

Widjaja E, Zamyadi M, Raybaud C, Snead OC, Smith ML. Impaired default mode network on resting-state FMRI in children with medically refractory epilepsy. AJNR Am J Neuroradiol 2013a; 34: 552–7.

Widjaja E, Zamyadi M, Raybaud C, Snead OC, Smith ML. Abnormal functional network connectivity among resting-state networks in children with frontal lobe epilepsy. AJNR Am J Neuroradiol 2013b; 34: 2386–92.

Yakushev I, Chetelat G, Fischer FU, Landeau B, Bastin C, Scheurich A, et al. Metabolic and structural connectivity within the default mode network relates to working memory performance in young healthy adults. Neuroimage 2013; 79: 184–90.